Effector-Stimulated Single Molecule Protein-DNA Interactions of a Quorum-Sensing System in *Sinorhizobium meliloti*

Frank Wilco Bartels,* Matthew McIntosh,† Alexander Fuhrmann,* Christoph Metzendorf,† Patrik Plattner,‡ Norbert Sewald,‡ Dario Anselmetti,* Robert Ros,* and Anke Becker†

*Experimental Biophysics and Applied Nanoscience, Department of Physics, †Institute for Genome Research and Systems Biology, Center for Biotechnology, and ‡Organic and Bioorganic Chemistry, Department of Chemistry, Bielefeld University, 33615 Bielefeld, Germany

ABSTRACT Intercellular communication by means of small signal molecules coordinates gene expression among bacteria. This population density-dependent regulation is known as quorum sensing. The symbiotic nitrogen-fixing bacterium *Sinorhizobium meliloti* Rm1021 possesses the Sin quorum sensing system based on *N*-acyl homoserine lactones (AHL) as signal molecules. Here, we demonstrate that the LuxR-type regulator ExpR binds specifically to a target sequence in the *sinRI* locus in the presence of different AHLs with acyl side chains from 8 to 20 carbons. Dynamic force spectroscopy based on the atomic force microscope provided detailed information about the molecular mechanism of binding upon activation by six different AHLs. These single molecule experiments revealed that the mean lifetime of the bound protein-DNA complex varies depending on the specific effector molecule. The small differences between individual AHLs also had a pronounced influence on the structure of protein-DNA interaction: The reaction length of dissociation varied from 2.6 to 5.8 Å. In addition, dynamic force spectroscopy experiments indicate that *N*-heptanoyl-DL-homoserine lactone binds to ExpR but is not able to stimulate protein-DNA interaction.

INTRODUCTION

Quorum sensing (QS) is a form of population density-dependent gene regulation controlled by low molecular weight compounds called autoinducers, which are produced by bacteria. QS is known to regulate many different physiological processes, including the production of secondary metabolites, conjugal plasmid transfer, swimming, swarming, biofilm maturation, and virulence in human, plant, and animal pathogens (reviewed in Gonzalez and Marketon (1) and Swift et al. (2)). Many QS systems involve *N*-acyl homoserine lactones (AHLs) as signal molecules (reviewed in Fuqua et al. (3)). These AHLs vary in length, degree of substitution, and saturation of the acyl chain (Fig. 1). Bacterial cell walls are permeable to AHLs, either by unassisted diffusion across the cell membrane (for shorter acyl chain length) or active transport (possibly for longer acyl chain length) (4). With the increase in the number of cells, AHLs accumulate both intracellularly and extracellularly. Once a threshold concentration is reached, they act as coinducers, usually by activating LuxR-type transcriptional regulators.

Sinorhizobium meliloti is an α-proteobacterium that fixes atmospheric dinitrogen to ammonia in a symbiotic association with certain genera of leguminous plants, including *Medicago, Melilotus*, and *Trigonella*. In *S. meliloti* Rm1021, a QS system consisting of the AHL synthase SinI and the LuxR-type AHL receptors SinR and ExpR was identified (5). SinI is responsible for production of several long-chain AHLs (C_{12}-HL – C_{18}-HL) (6). The presence of a second QS system, the Mel system, controlling the synthesis of short-chain AHLs (C_6-HL – C_8-HL) was suggested (6). In addition to SinR, five other putative AHL receptors, including ExpR, were identified (7). As originally described for the model QS LuxI/LuxR system of *Vibrio fischeri* (8) and demonstrated for the TraR-AHL complex of *Agrobacterium tumefaciens* whose crystal structure was resolved (9), it is assumed that the LuxR-type regulators of *S. meliloti* are activated by binding of specific AHLs. Once activated, the expression of target genes is regulated by binding upstream of the promoter regions of these genes (10). The first target genes identified for the *S. meliloti* Sin system were the *exp* genes mediating biosynthesis of the exopolysaccharide galactoglucan. The expression of the *exp* genes not only relies on a sufficient concentration of Sin system-specific AHLs but also requires the presence of the LuxR-type AHL receptor ExpR (7,11). Data of transcriptomics and proteomics approaches suggested that the majority of target genes of the Sin system is controlled by ExpR (12,13). The *S. meliloti* Rm1021 wild-type strain carries an inactive *expR* gene due to disruption of its coding region by insertion element IS*Rm*2011-1 (7). However, the spontaneous dominant mutation *expR101* resulting from precise reading frame-restoring excision of the insertion element from the coding region unraveled the role of *expR* in regulation of galactoglucan biosynthesis (7). ExpR is highly homologous to the *V. fischeri* LuxR. Activated LuxR-type regulators usually bind to a consensus sequence known as the lux box, typically located upstream of the promoters of its target genes (10). However, the DNA binding site of ExpR has not yet been identified.

During the last decade, dynamic force spectroscopy (DFS) has developed into a highly sensitive tool for investigation of the interaction of single biomolecules (14), from complementary DNA strands (15) to ligand-receptor pairs (16–20) and cell adhesion molecules (21). Only most recently has

Submitted January 25, 2006, and accepted for publication January 26, 2007.

Address reprint requests to Robert Ros, Tel.: 49-(0)521-106-5388; Fax: 49-(0)521-106-2959; E-mail: rros@physik.uni-bielefeld.de.

0006-3495/07/06/4391/10 $2.00

doi: 10.1529/biophysj.106.082016

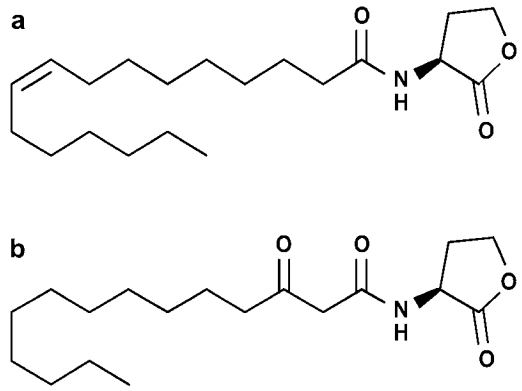

FIGURE 1 AHLs. Of the synthesized AHLs, those with modifications in the acyl side chain are shown: (*a*) *N*-[(9Z)-hexadec-9-enoyl]-L-homoserine lactone ($C_{16:1}$-HL) and (*b*) *N*-(3-Oxotetradecanoyl)-L-homoserine lactone (oxo-C_{14}-HL).

protein-DNA interaction come under survey by DFS (22–26). In particular, DFS data have proven to complement the information gained from conventional molecular biology experiments in a detailed study of DNA binding of the regulator ExpG-activating transcription of the *exp* genes (25).

Most DFS experiments use either optical tweezers or an atomic force microscope (AFM) to measure dissociation forces of single bound complexes in the piconewton range. The molecular binding partners are attached to the micro- or nanoscale force sensor and a sample holder, respectively, by covalent chemistry. When both parts are brought into close contact, a specific bond between the individual molecules can form. By increasing the distance again, the bond is loaded until it finally severs. This event yields a discrete dissociation force. By systematic variation of the externally applied load, information on the energy landscape of the interaction can be derived (27,28): the equilibrium rate of dissociation, the mean lifetime of the bond, and the length of the dissociation path.

In this study, we identified the DNA binding site of ExpR in the region upstream of *sinI* and a spectrum of AHLs stimulating the DNA-binding activity of ExpR. Individual bound complexes were analyzed by DFS and kinetic parameters, which delicately depend on minute differences between effector molecules, were derived.

MATERIALS AND METHODS

Bacterial strains, plasmids, and growth conditions

Bacterial strains used in this study have the following phenotypes: *Escherichia coli* M15[pREP4] (Qiagen, Hilden, Germany) Nal^s, Str^s, Rif^s, Thi^-, Lac^-, Ara^+, Gal^+, Mtl^-, F^-, $RecA^+$, Uvr^+, Lon^+; *S. meliloti* Rm1021 (29) Sm^r, Nal^r, $expR^-$; *S. meliloti* Rm1021 *expR101* (Rm8530) (30) Sm^r, Nal^r, $expR^+$. *S. meliloti* strains were incubated at 30°C in Luria-Bertani (LB) medium supplemented with 2.5 mM $MgSO_4$ and 2.5 mM $CaCl_2$ (LB/MC) or tryptone-yeast (TY) medium (31). *E. coli* strains were incubated at 37°C in LB medium. Antibiotics were added at the following concentrations ($\mu g/ml^{-1}$): for *S. meliloti*: gentamycin (Gm) 40, nalidixic acid (Nal) 10, streptomycin (Sm) 600; for *E. coli*: ampicillin (Ap) 100, gentamycin (Gm) 10.

Plasmid construction

Primers (AAAAGAATTCGAATATTACGTTGCTCGTACAGT and AATTAAGCTTGCTCTAACTTCTACAGGACT) (restriction sites are underlined) deduced from the *S. meliloti* Rm1021 sequence were used for polymerase chain reaction (PCR) amplification of the *expR* coding region. As template, genomic DNA was extracted from Rm8530, which carries the functional *expR101* allele (7). A plasmid encoding an ExpR derivative with a six-histidine N-terminal tag was constructed as follows. The PCR product was digested with *Bam*HI and *Hin*dIII and ligated into vector pWH844 (pQE-9 derivative, lacIq, 5.0 kb, Ap^r, T5, $(His)_6$-tag) (32). Expression of this construct resulted in an ExpR protein with six N-terminally fused histidine residues [$(His)_6$-ExpR]. Both *expR* and $(his)_6$-*expR* preceded by the Shine-Dalgarno sequence derived from the multiple cloning site of vector pWH844 were also cloned into the broad host range vector (33), using primers TTAAGGATCCAATATTACGTTGCTCGTACA and AATTAAGCTTGCTCTAACTTCTACAGGACT and the restriction enzymes *Bam*HI and *Hin*dIII. The resulting plasmids were transferred to *S. meliloti* Rm1021 by *E. coli* S17-1-mediated conjugation (34).

Expression and purification of protein

$(His)_6$-ExpR was overexpressed in *E. coli* M15 and purified under nondenaturing conditions according to the QIAexpressionist handbook. Upon induction with 0.02 mM ITPG, the LB cell culture (800 mL) was grown at 25°C overnight. Cell pellet was harvested and resuspended in a 1/20 volume of lysis buffer containing 0.5% Triton-X 100, 50 mM Tris, pH 8.0, 0.5 M NaCl, 20 mM imidazole, 0.5 mM PMSF, and 0.5 mg DNase (SERVA, Heidelberg, Germany). Cell breakage was performed using a French Pressure Cell at 1380 psi. Cell debris was removed by centrifugation at 44,000 × *g*, and the supernatant was loaded onto a 10 mL volume Ni-NTA affinity column (Qiagen). The column was washed with buffer (60 mL) containing 0.5% Triton-X 100, 50 mM Tris, pH 8.0, 0.5 M NaCl, and 20 mM imidazole, followed by a second buffer (50 mL) containing 50 mM Tris, pH 8.0, 0.5 M NaCl, and 20 mM imidazole. Elution of the protein was by loading a buffer with an imidazole gradient (0.02–1.0 M, 50 mL) containing 50 mM Tris, pH 8.0, and 0.5 M NaCl. Fractions (2 mL) were collected and analyzed with sodium dodecylsulfate-polyacrylamide gel electrophoresis, and the protein concentration estimated using the Bio-Rad Protein Assay (Bio-Rad Laboratories, München, Germany). Protein was stored in the elution buffer at 4°C and was stable for at least several months.

DNA labeling

The DNA probe used in the electrophoretic mobility shift assays (EMSAs), the DNA footprinting assay, and the AFM experiments was derived from a 216-bp region (UpsinI) that included 31 bp of the 3′ end of *sinR*, the 156-bp intergenic region between *sinR* and *sinI*, and 29 bp of the 5′ end of *sinI*. UpsinI was PCR amplified using the flanking primers ATATAAGCTTTGTTCGACATGCTCTGATCC and ATATGAATTCCGACCGTTTCCGTTCACTAT and cloned into *Hin*dIII and *Eco*RI digested pUC18 (restriction sites in primer sequences are underlined). When the universal primers AGCGGATAACAATTTCACACAGGA and GTTTTCCCAGTCACGAC were used in a PCR with the UpsinI cloned into pUC18 as the template, a 313-bp fragment was amplified. The DNA fragment was labeled using PCR amplification in which the 5′ primer contained either 5′Cy3 (for EMSAs), 5′fluorescein (for DNA footprinting assays), or 5′SH for AFM measurements.

$UpsinI_{Cy3}$ fragment carrying point mutations at positions −106 (T replaced by G), −104 (T replaced by G), and −99 (G replaced by C) upstream of the *sinI* start codon was generated by PCR using two additional

internal primers, pmut6upsinIfwd (GATTCCCCCACAAAGCGATTGCGAAAAAATGAGGAAATAA) and pmut6upsinIrev (CTCATTTTTTCGCAATCGCTTTGTGGGGGAATCTG). These primers bind to the ExpR protected region and contain the three bp alterations and complementary regions.

The internal primers were used in two separate PCR steps in combination with the flanking primers. The products of these PCRs were purified and combined and, upon annealing at the complementary regions, formed the template for the final PCR in which the flanking Cy3-labeled primers were used.

Synthesis of effector molecules

For the synthesis of AHLs with saturated side chains, fatty acids were converted into the corresponding acid chloride. They were slowly added to an ice cold solution of homoserine lactone hydrobromide and two equivalents of pyridine in methanol. After stirring for 3 h at room temperature, the solvent was removed in the vacuum and the residues dissolved in ethyl acetate. *N*-Octanoyl-L-homoserine lactone (C_8-HL), *N*-dodecanoyl-L-homoserine lactone (C_{12}-HL), *N*-pentadecanoyl-L-homoserine lactone (C_{15}-HL), *N*-octadecanoyl-L-homoserine lactone (C_{18}-HL), and *N*-eicosanoyl-L-homoserine lactone (C_{20}-HL) were synthesized in this manner. *N*-[(9Z)-hexadec-9-enoyl]-L-homoserine lactone ($C_{16:1}$-HL, Fig. 1 *a*) was prepared from homoserine lactone hydrobromide and palmitoleic acid in a water-acetonitrile mixture by addition of base and 1-ethyl-3-(3-dimethylamino-propyl) carbodiimide hydrochloride (EDC). After 18 h the product was extracted from the reaction mixture using methylene chloride.

A previously reported synthesis protocol for β-keto esters was followed to prepare *N*-(3-oxotetradecanoyl)-L-homoserine lactone (oxo-C_{14}-HL, Fig. 1 *b*) (35). One equivalent each of *N*,*N*′-dicyclohexyl carbodiimide (DCC), 4-(dimethylamino)pyridine, and 2,2-dimethyl-1,3-dioxan-4,6-dione was added to a solution of lauric acid in methylene chloride. After stirring for 18 h at room temperature the solvent was evaporated. The residue was resuspended in ethyl acetate and washed with 1 M hydrochloric acid and saturated sodium chloride solution. The solvent was evaporated and the solid residue dissolved in acetonitrile and homoserine lactone was added. The dispersion was heated to reflux for 3 h. Evaporation of acetonitrile was followed by addition of ethyl acetate and aqueous workup. *N*-(3-oxohexadecanoyl)-L-homoserine lactone (oxo-C_{16}-HL) was synthesized following an analogous protocol.

All synthesized AHL molecules were purified by reversed-phase high performance liquid chromatography (HPLC) with acetonitrile/water/TFA gradients or by column chromatography with organic eluents and their structures were confirmed by mass spectrometry (MS) and proton NMR spectroscopy. The following substances were purchased from Sigma-Aldrich (München, Germany): *N*-hexanoyl-DL-homoserine lactone (C_6-HL), *N*-heptanoyl-DL-homoserine lactone (C_7-HL), *N*-(3-oxooctanoyl)-DL-homoserine lactone (oxo-C_8), *N*-decanoyl-DL-homoserine lactone (C_{10}-HL), *N*-tetradecanoyl-DL-homoserine lactone (C_{14}-HL), and palmitoleic acid. Crude AHL extract from *S. meliloti* Rm1021 was obtained as described by Marketon et al. (6).

Electrophoretic mobility shift assays

The EMSA protocol has been described (22,25). The Cy3-labeled DNA wild-type fragment ($UpsinI_{Cy3}$) or the mutated $UpsinI_{Cy3}$ fragment were mixed with purified $(His)_6$ExpR in a reaction buffer containing ~0.25 nmol of sonicated herring testes DNA in a final volume of 20 μL of DNA-binding buffer (20 mM Tris-HCL, pH 8.0, 50 mM KCl). $(His)_6$ExpR was included at 0.4 mM, and AHLs were added to a final concentration of 10 μM. The reactions were incubated at 24°C for 20 min. Loading buffer (5 μL, 78% glycerol) was added, and the reaction mixtures were loaded onto a 2% agarose gel at 4°C. After electrophoresis at 5 V/cm for 2 h, gel images were acquired using a Typhoon 8600 Variable Mode Imager (Amersham Bioscience, Freiburg, Germany).

DNA footprinting assays

The 5′fluorescein-labeled DNA fragment (UpsinI) was incubated with and without $(His)_6$ExpR under conditions similar to the EMSA assay, except that benzonase (Sigma-Aldrich) was included, ranging 3–0.004 U, and the digestion mixture included 0.25 mM $MgCl_2$ and 0.125 mM $CaCl_2$. Sequencing products and fragments resulting from benzonase digest were separated on an ABI PRISM 377 DNA Sequencer (Applied Biosystems, Foster City, CA).

Reverse transcription and real-time PCR

Two independent cultures of each strain were grown in TY medium and harvested at optical density (600 nm) 1.0. RNA was extracted using the RNeasy Mini Kit (Qiagen). Reverse transcription and real-time PCR (qRT-PCR) were carried out using the QuantiTect SYBR Green PCR kit (Qiagen) and a continuous fluorescence detector (DNA Engine OPTICON, Bio-Rad Laboratories) as described previously (36). Quantification was performed with the Opticon Monitor analysis software version 1.8. Cycle threshold values of the gene SMc02461, found to be substantially expressed at similar levels under a number of different conditions (36), were used as a reference for normalization. The following primers were used: for *expE1* ATGGTGACGACTTGCTGTTC and GAGGTCGATGACGACATTGC; for *expR* CCGCATGAGAATCCGCTGAG and CCGTCGAAGAGGCCATGATT; for *sinI* CAAGATTCGTGGCTCCCTCA and ATGGTGACCTGGTTCGATGC; and for *smc02461* CTTGCGGTTGTCGTTGACG and TTCATCAACGAGATTGCCGA.

Sample surface and AFM tip modification

For force spectroscopy measurements, sample surfaces and AFM tips were functionalized as described previously (22). Briefly, Si_3N_4 cantilevers (MSCT-AUHW, Veeco Instruments, Santa Barbara, CA, or OMCL-TR400PSA-HW, Olympus, Tokyo, Japan) were first activated by dipping for 10 s in concentrated nitric acid and silanized in a solution of 2% aminopropyl-triethoxysilane (Sigma-Aldrich) in dry toluene for 2 h. After washing with toluene, the cantilevers were incubated with 1 mM *N*-hydroxysuccinimide-poly(ethylene glycol)-maleimide (Shearwater Polymers, Huntsville, AL) in 0.1 M potassium phosphate buffer, pH 8.0, for 30 min at room temperature. After washing with phosphate buffer, the cantilevers were incubated with 10 ng/μl of the DNA target sequence (see above) bearing a sulfhydryl label in binding buffer solution (100 mM K_2HPO_4/KH_2PO_4, pH 7.5) overnight at 4°C. The cantilevers were washed with binding buffer and used for force spectroscopy experiments. Modified tips were usable for at least 1 week if stored at 4°C.

Mica surfaces (Provac AG, Balzers, Liechtenstein) were silanized with aminopropyltriethoxysilane in an exsiccator and incubated with 4 μM $(His)_6$ExpR protein and 20 μM bis(sulfosuccinimidyl)suberate-sodium salt (Sigma-Aldrich) in 0.1 M potassium phosphate buffer, pH 7.5, for 1 h at 4°C. The sample was washed with binding buffer afterward. Modified surfaces were stable for at least 2 days if stored at 4°C. A scheme of the experimental setup is shown in Fig. 3 *a*.

Dynamic force spectroscopy

Force spectroscopy measurements were performed with a home-built force spectroscopy setup based on a commercial AFM (Multimode, Veeco Instruments) at 25°C. Acquisition of the cantilever deflection force signal and the vertical movement of the piezo electric elements was controlled by a 16-bit AD/DA card (PCI-6052E, National Instruments, Austin, TX) and a high-voltage amplifier (600H, NanoTechTools, Echandens, Switzerland) via home-built software based on Labview (National Instruments). The deflection signal was low-pass filtered (<6 kHz) and box averaged by a factor of 10, giving a typical experimental data set of 2500 points per force-distance curve.

The spring constants of all AFM cantilevers were calibrated by the thermal fluctuation method (37) with an absolute uncertainty of ~15%. Spring constants of the cantilevers used ranged from 8 pN/nm to 16 pN/nm (Veeco) and from 18 to 26 pN/nm (Olympus).

For loading rate-dependent measurements, the retract velocity of the piezo was varied while keeping the approach velocity constant. The measured force-distance curves were analyzed with a MATLAB program (The MathWorks, Natick, MA) and corrected to display the actual molecular distances calculated from the z piezo extension. To obtain the loading rate, the retract velocity was then multiplied by the elasticity of the molecular system, which was determined from the slope of the corrected force-distance curves on the last 20 data points before the dissociation events.

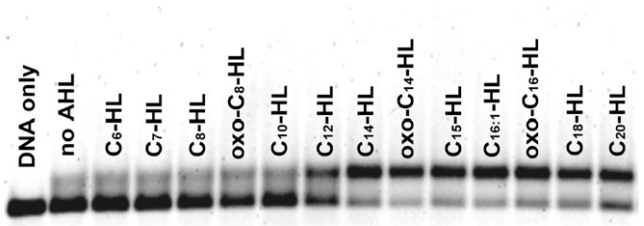

FIGURE 2 AHL-dependent DNA binding of purified $(His)_6$ExpR. A Cy3-labeled probe derived from the *sinR-sinI* intergenic region was used in the gel shift assay. AHLs were included in the binding reaction at 10 μM.

RESULTS AND DISCUSSION

$(His)_6$ExpR activated by AHLs specifically binds to the *sinR-sinI* intergenic region

The *S. meliloti* ExpR protein shows homologies to LuxR-type AHL receptors, which have a C-terminal DNA binding and an N-terminal AHL binding domain that inhibits the activity of the C-terminal domain in the absence of the autoinducer (38). Marketon et al. (5) reported evidence for a positive *sinR*-dependent feedback regulation of *sinI* expression. A comparison of *sinI* mRNA levels in the $expR^-$ strain Rm1021 and the $expR^+$ strain Rm1021 *expR101* at a culture $O.D._{600}$ of 1.0 showed a 4.3-fold increase, indicating a positive regulation of *sinI* expression by ExpR. Moreover, we identified a lux box-like sequence (TATAGTACATGT) 70 bp upstream of *sinI* which constitutes a putative binding site for the LuxR-type regulators ExpR and SinR. Therefore, the *sinR-sinI* intergenic region was selected as a candidate for an ExpR target sequence.

For binding assays ExpR protein was expressed in *E. coli* with an N-terminal His-tag ($(His)_6$ExpR). Addition of AHLs during expression in *E. coli* strain M15 was not required for either stability or solubility. Binding of purified $(His)_6$ExpR protein to a 313-bp fragment was analyzed in ensemble experiments by EMSA and at the single molecule level by force spectroscopy. This DNA fragment included 97-bp flanking sequences derived from the pUC18 vector, 31 bp of the 3′ end of *sinR*, the 156-bp *sinR-sinI* intergenic region, and 29 bp of the 5′ end of *sinI*. Various AHLs were tested for stimulation of the ExpR DNA-binding activity. These included AHLs found to be produced by bacteria but also AHLs which so far have not been found to be synthesized by bacteria, namely C_{15}- and C_{20}-HLs. $(His)_6$ExpR showed minimal levels of binding to the DNA in the absence of AHL or in the presence of 10 μM of the short chain C_6-, C_7-, C_8-, oxo-C_8-, or C_{10}-HLs (Fig. 2). In the presence of 10 μM C_{14}-, oxo-C_{14}-, C_{15}-, $C_{16:1}$-, oxo-C_{16}-, C_{18}-, or C_{20}-HLs maximum stimulation of binding was observed, whereas C_{12}-HL stimulated binding to a lesser extent (Fig. 2). No binding was observed in control experiments with DNA fragments derived from the Epstein-Barr virus nuclear antigen (EBNA-1) gene (22) (data not shown). Furthermore, activation of the DNA-binding activity of ExpR was not achieved by addition of palmitoleic acid, showing that the homoserine part of the AHLs is essential. These results indicate that AHL-activated $(His)_6$ExpR binds specifically to the *sinR-sinI* intergenic region.

To investigate the ExpR-DNA interaction on a single molecule basis, the binding partners were covalently bound to the sample surface and to the AFM tip, respectively. The DNA fragment was attached to the tip via a polymer spacer, whereas the $(His)_6$ExpR protein was immobilized on the surface by a short linker molecule coupled to one of the 11 ExpR lysines (Fig. 3 *a*). When the tip was approached to and retracted from the surface, the flexibility of the polymer chain allowed the DNA molecules to access the binding domains of immobilized proteins. By plotting the force acting on the AFM tip against the vertical position (given by the extension of the piezo actuator), dissociation events can be identified by a characteristic stretching of the polymer spacer before the point of bond rupture (where the tip snaps back to zero force). A typical force-distance curve is shown in Fig. 3 *b*. The dissociation forces from multiple approach-retract cycles under a single retract velocity were combined in a histogram. The total dissociation probability (events/cycles) remained below 0.5% for the bare protein-DNA system in buffer solution, the histogram consisting of scattered events (Fig. 3 *c*). The background signal, i.e., a series of measurements with a functionalized surface and an AFM tip without any DNA but prepared as normal in all other respects, was checked and revealed no dissociation events. The profile changed drastically when AHL was added to give a final concentration of 10 μM (oxo-C_{14}-HL in the case of Fig. 3 *d*). The total dissociation probability increased to 8%–10%, and the dissociation forces form a distribution of almost Gaussian shape. The mean value of the Gaussian then equals the most probable dissociation force, with statistical errors given by standard deviation ($2\sigma/\sqrt{N}$ for 95.4% confidence level). Data from this experiment indicate that ExpR binds to DNA even in the absence of any effector due to unspecific attraction (e.g., electrostatic forces) but the probability of binding is highly increased in the presence of a proper effector.

Competition experiments were performed to address whether the observed binding forces are specific. Fig. 4 *a* shows a histogram of the dissociation forces similar to Fig. 3 *d* but activated by 10 μM $C_{16:1}$-HL. After adding free DNA fragments (10 ng/μL) to the buffer solution, a

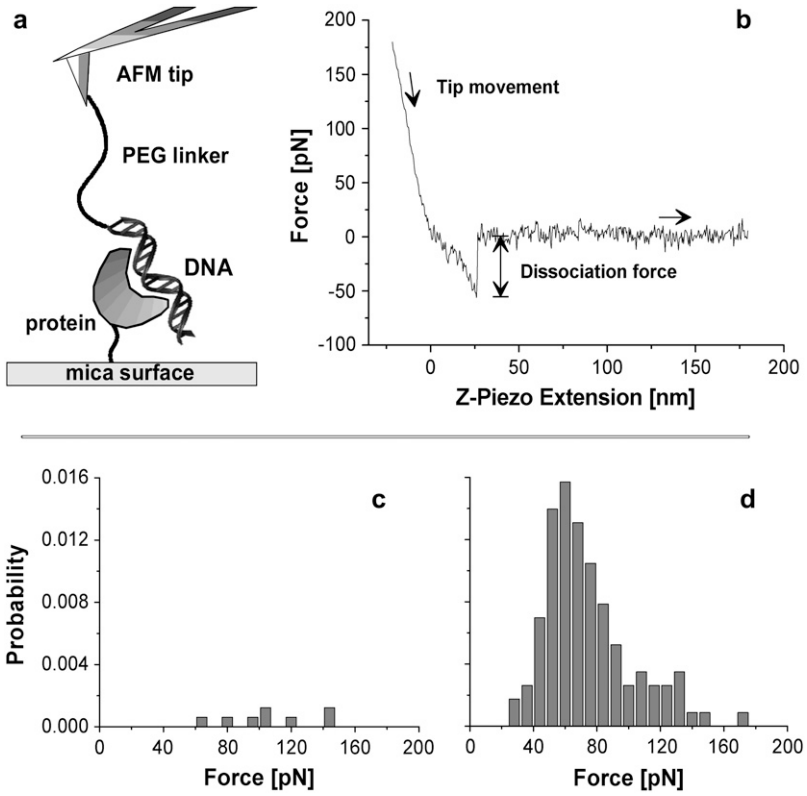

FIGURE 3 Force spectroscopy measurements. (*a*) The experimental setup consists of a Si_3N_4 AFM tip with DNA fragments attached via poly(ethylene glycol) spacer molecules and a flat mica surface on which the $(His)_6$ExpR proteins are immobilized. (*b*) Typical force-distance curve for the retraction of the tip from the sample surface at constant velocity. (*c*) Distribution of dissociation forces for the DNA-$(His)_6$ExpR complex without effector (at v = 2000 nm/s) and (*d*) after adding 10 μM of oxo-C_{14}-HL.

distinct reduction of the binding probability was observed (Fig. 4 *b*). Washing with DNA-free buffer solution restores the initial unbinding probability (data not shown). In additional control experiments, the DNA-binding fragment on the AFM tip is replaced by EBNA-DNA fragments (EBNA) which lack the binding sequence. With this setup and in the presence of 10 μM $C_{16:1}$-HL, nearly no binding could be observed at all (Fig. 4 *c*). These results clearly prove that the binding of the peptide with the native sequence actually takes place specifically at the binding sequence on the DNA.

AFM force spectroscopy proved to be a sensitive tool to determine the influence of different effector molecules. Of the seven effectors tested, C_8-HL, C_{10}-HL, C_{12}-HL, oxo-C_{14}-HL, $C_{16:1}$-HL, and C_{18}-HL stimulated protein-DNA binding (see Fig. 7 for the most probable dissociation forces under different velocities). Only C_7-HL caused no noticeable increase in activity when added to the buffer solution (see Fig. 8 *a*).

Complementation of an *expR* mutant confirms the activity of $(His)_6$ExpR in vivo

To test the functionality of $(His)_6$ExpR in vivo, the native *expR* gene and the $(his)_6$*expR* fusion gene were cloned into the broad host range vector pJN105. Both plasmids were introduced to Rm1021, a strain in which the endogenous *expR* is not functional. After reverse transcription, real time PCR was applied to measure the abundance of RNA transcripts derived from *expR* and the galactoglucan biosynthesis gene *expE1*. Stimulation of *expE2* expression has been previously found to be an indicator for ExpR activity (7,11). This gene is located just downstream of *expE1* which is the first gene of the *expE* operon (39).

As a control, *expR* and *expE1* expression was compared in the $expR^+$ revertant Rm1021 *expR101* and the Rm1021 $expR^-$ wild-type strain carrying the empty pJN105 vector. Compared to *expE1* expression in strain Rm1021/pJN105, both *expR* and $(his)_6$*expR* complemented strains Rm1021/pJQR*expR*, and Rm1021/pJQR$(his)_6$*expR* showed stimulation of *expE1* expression (Table 1). Complementation of the Rm1021 $expR^-$ wild-type strain by expression of the $(his)_6$*expR* gene demonstrated that the $(His)_6$ExpR protein functions in vivo.

Binding of $(His)_6$ExpR protects a 30-bp region including a lux box-like sequence against nucleolytic digestion

Benzonase footprinting was applied to identify the specific binding site of $(His)_6$ExpR upstream of *sinI*. In the presence of 10 μM oxo-C_{14}-HL, $(His)_6$ExpR protected a 26-bp region adjacent to a downstream 13-bp lux box-like sequence (Fig. 5). EMSA experiments with subfragments of the *sinI-sinR* intergenic region indicated that a 46-bp sequence immediately upstream of the putative lux box is sufficient for binding of $(His)_6$ExpR (data not shown). This indicates that

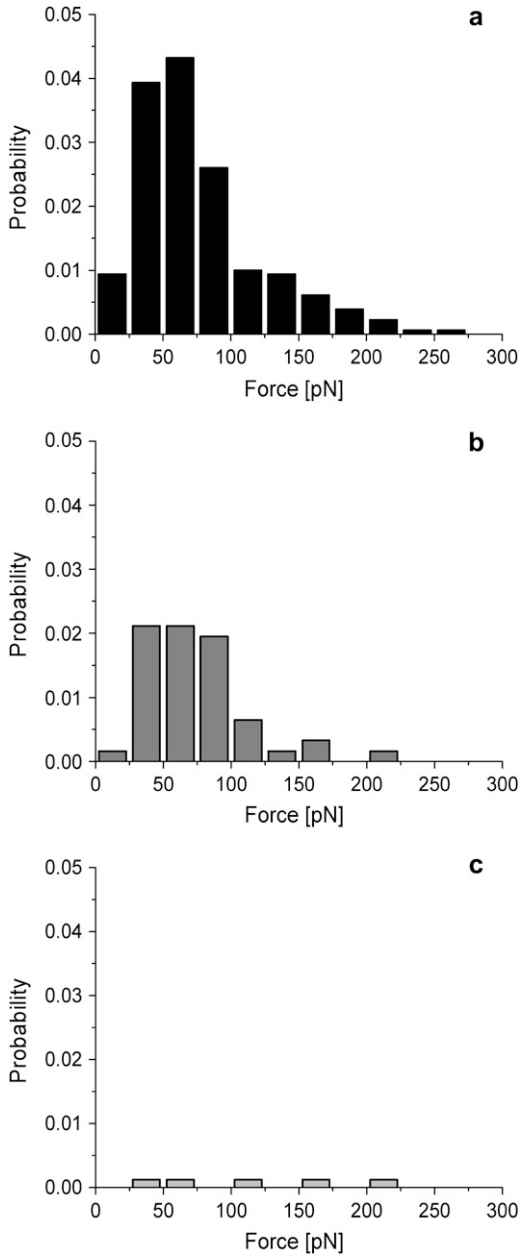

FIGURE 4 Force spectroscopy control experiments. (*a*) Distribution of the dissociation forces of DNA-$(His)_6$ExpR complexes in the presence of 10 μM $C_{16:1}$-HL. (*b*) After adding free DNA fragment (10 ng/μL) as competitor. (*c*) Additional control experiment with EBNA-DNA immobilized on the AFM tip and $C_{16:1}$-HL-activated $(His)_6$ExpR.

the $(His)_6$ExpR binding site is located just upstream of the putative lux box. The assay was repeated where $(His)_6$ExpR was replaced with native ExpR in crude *E. coli* extract, resulting in protection of the same 26-bp DNA region (results not shown). Directed mutation of the ExpR binding site, involving three bps (positions T_{-106} replaced by G_{-106}, T_{-104} replaced by G_{-104}, and G_{-99} replaced by C_{-99} upstream of the *sinI* start codon) within the benzonase protected region (Fig. 5), resulted in the complete absence of binding by $(His)_6$ExpR in the presence of oxo-C_{14}-HL (Fig. 6). This finding further supports the involvement of the protected region in specific binding to ExpR.

TABLE 1 Gene expression of *expR* and *expE1* derived from qRT-PCR

Gene	Rm1021 *expR101* vs. Rm1021/pJN105	Rm1021/pJQR*expR* vs. Rm1021/pJN105	Rm1021/pJQR(his)$_6$*expR* vs. Rm1021/pJN105
expR	22200	55600	79333
expE1	55	37	38

Values indicate fold changes of RNA levels of *expR* and *expE1* in strains Rm1021 *expR101*, Rm1021/pJQR*expR*, and Rm1021/pJQR(his)$_6$*expR*. The Rm1021 *expR*$^-$ wild-type carrying the empty vector pJN105 (Rm1021/pJN105) was used as reference. Transcript levels of gene SMc02461 were used for normalization. The error of the calculated normalized gene expression was $<$20%. This experiment was repeated three times with independent cultures.

Dynamic force spectroscopy reveals that molecular interaction parameters of AHL-activated ExpR vary with different AHLs

The influence of the six effectors which stimulated ExpR-DNA binding was then studied in detail by DFS measurements. For each effector, typically 80–150 dissociation events of the protein-DNA complex (1000–2000 approach/retract cycles) were recorded at 5–9 different retract velocities ranging from 100 nm/s to 6000 nm/s while the approach velocity was kept constant at 2000 nm/s. These resulted in loading rates r = molecule elasticity $\times$ retract velocity in the range between 220 pN/s and 44000 pN/s.

When the dissociation forces are plotted against the corresponding loading rates on a logarithmic scale, a characteristic linear dependence becomes apparent (Fig. 7). This is in accordance with force spectroscopy theory (27,28), the fitting function being given as

$$F = \frac{k_B T}{x_\beta} \ln \frac{x_\beta r}{k_B T k_{off}} ,$$

wherein F is the most probable dissociation force, k_BT = 4.114 pN nm (at 298 K) is a Boltzmann factor, r is the loading rate, and k_{off} is the thermal off-rate under zero load. The molecular parameter x_β defines the distance between the minimum of the potential well of the bound state and the maximum of the energy barrier separating the bound state from the free state along the reaction coordinate. This is often interpreted as the depth of the binding pocket (see Merkel et al. (28) for a thorough analysis). By extrapolating the linear fit to the state of zero external force, the thermal off-rate k_{off} of the ligand-receptor complex can be derived. The molecular interaction parameters gained from the experimental data in Fig. 7 are summarized in Table 2.

The different effectors showed a distinct influence on the kinetics and structure of the ExpR-DNA binding. Most off-rates were close to $k_{off} = 2\ s^{-1}$, which corresponds to a mean

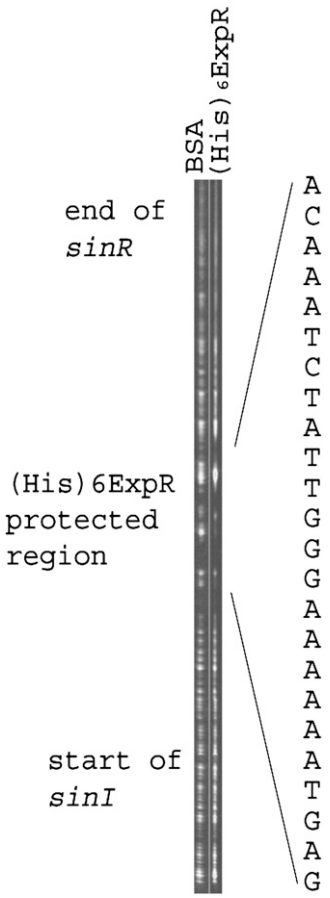

FIGURE 5 Benzonase protection of an upstream region of *sinI* by oxo-C_{14}-HL-stimulated $(His)_6$ExpR. A fluoroscein-labeled DNA fragment derived from the *sinR-sinI* intergenic region was preincubated in the presence of 10 μM oxo-C_{14}-HL with either 2 μM bovine serum albumin (lane 1) or with 2 μM $(His)_6$ExpR (lane 2) and was then partially digested with benzonase, as described in Materials and Methods. The DNA sequence protected by $(His)_6$ExpR is indicated on the right side of the figure. An indication of the position of the footprint relative to the flanking genes and the lux box homolog is indicated on the left of the diagram.

lifetime of ~0.5 s for the bound protein-DNA complex. The notable exceptions are C_8-HL, which caused an off-rate of $k_{off} = 0.5\ s^{-1}$ ($\tau = 2.3 \pm 0.8$ s), and C_{12}-HL with $k_{off} = 5.4\ s^{-1}$ ($\tau = 0.19 \pm 0.04$ s). The measured reaction length x_β indicates three different states as well: the long-chain AHLs (oxo-C_{14}-HL, $C_{16:1}$-HL, and C_{18}-HL) center around $x_\beta \sim 4.0$ Å, whereas the short-chain AHLs (C_8-HL and C_{10}-HL) tend to higher values at $x_\beta \sim 5.5$ Å, and C_{12}-HL has a strikingly low reaction length of $x_\beta \sim 3$ Å.

The lifetime of the ExpR-AHL complex exceeds the lifetime of the protein-DNA complex

Why is C_7-HL not able to stimulate protein-DNA interaction (Fig. 8 *a*)? One likely explanation would be that it does not bind to the ExpR protein. But this is not the case. Even after

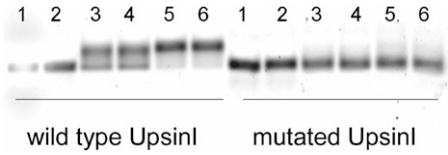

FIGURE 6 AHL-dependent DNA binding of purified $(His)_6$ExpR to the Cy3-labeled UpsinI wild-type fragment and the UpsinI fragment carrying point mutations. The mutated UpsinI fragment contains three altered bps at positions −106 (T replaced by G), −104 (T replaced by G), and −99 (G replaced by C) upstream of the *sinI* start codon. Lanes 1 and 2, UpsinI only; lanes 3 and 4, UpsinI with $(His)_6$ExpR; lanes 5 and 6, UpsinI with $(His)_6$ExpR and oxo-C_{14}-HL.

C_7-HL was removed from both the sample surface and the AFM tip by multiple washing steps with AHL-free buffer solution over the course of 1 h, addition of C_{12}-HL yielded very few dissociation events (Fig. 8 *b*). It seems that most proteins retained a C_7-HL effector which inhibited activation by C_{12}-HL. This suggests that, although C_7-HL binds to the ExpR protein, it is not able to change its conformation into an active state. This is a further indication that the chemical structure of a particular effector has a strong influence on the sterics of the ExpR protein and thereby on the kinetics of possible protein-DNA interactions.

The aforementioned experiment suggests a long lifetime of the C_7-HL effector-protein complex, resulting in an effective inhibition of activation of ExpR by C_{12}-HL. We performed an additional experiment in which C_{12}-HL was the first AHL added, which showed its usual degree of activity with a fresh protein sample (Fig. 8 *c*). As in the previous experiment, sample surface and AFM tip were washed multiple times over the course of 1 h before the addition of the second AHL, C_7-HL. Although the binding probability was marginally reduced after the washing step (Fig. 8 *d*), the system still showed a considerable degree of activity in the presence of C_7-HL. In contrast to the lifetime of the protein-DNA complex (which is $\tau = 185 \pm 35$ ms in the case of C_{12}-HL, see Table 2), the lifetime of the protein-effector bond seems to be much longer. ExpR-DNA kinetics can therefore be regarded as independent from AHL-ExpR kinetics, indicating that only the structural change of the protein induced by a particular AHL effector governed the properties of ExpR-DNA interaction in the DFS experiments.

CONCLUSION

Unlike the *A. tumefaciens* TraR LuxR-type QS regulator (40,41), $(His)_6$ExpR did not require the addition of AHLs during expression in *E. coli* for either stability or solubility. AHLs were required for correct folding of TraR and completely embedded in a narrow cavity of the protein (9). Removal of AHLs bound to the *V. fischeri* LuxR through competition with halogenated furanones resulted in rapid degradation of LuxR, indicating that the signal molecules are

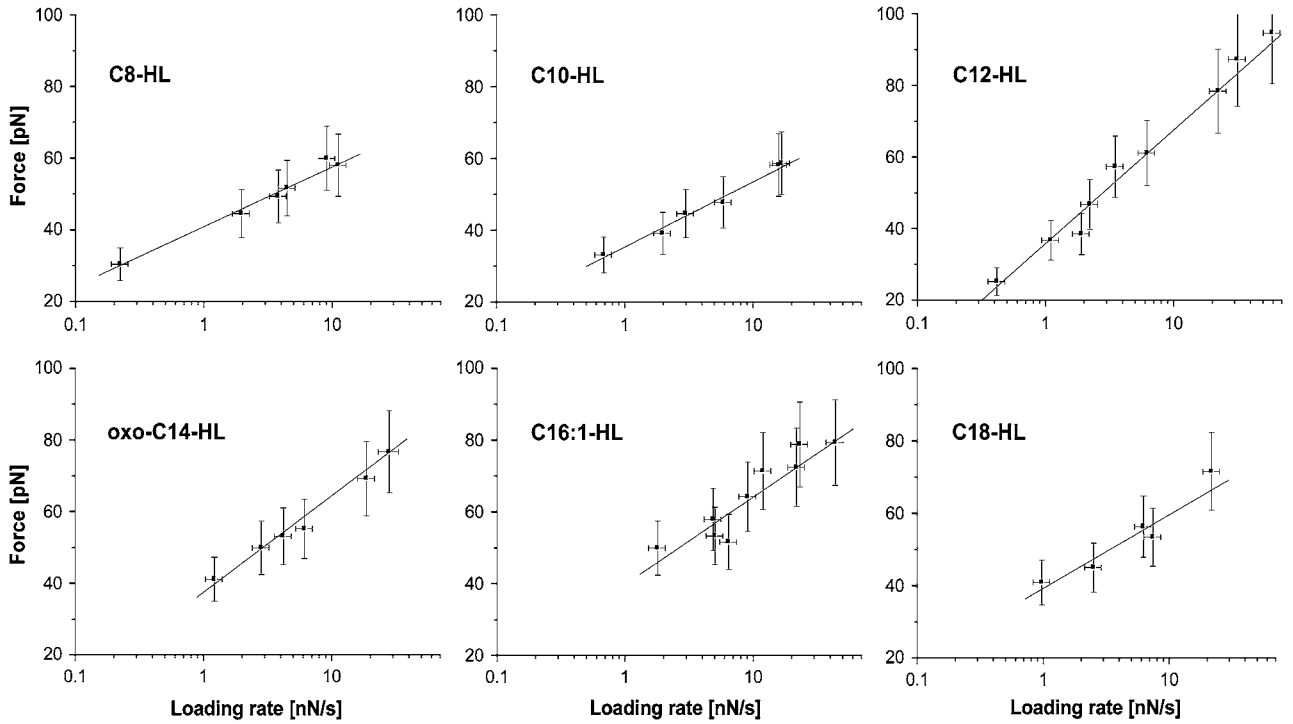

FIGURE 7 DFS. Dissociation forces depend on the natural logarithm of the loading rate, r, with r = molecule elasticity × retract velocity. By systematical variation of the retract velocity, complexes formed by the $(His)_6$ExpR protein and its DNA target sequence under the influence of different effectors where probed. Extrapolating the line fit to the state of zero external force yields the natural thermal off-rate k_{off} for each data set. The derived values are summarized in Table 2.

essential for the stability of LuxR not only during folding but also for the duration of its lifetime (42). Due to its stability in the absence of AHLs the *S. meliloti* ExpR protein is an ideal model system for analysis of the AHL activation spectrum of a LuxR-type QS receptor.

A DNA binding site of ExpR was identified upstream of the AHL synthase gene *sinI*. The interaction is stimulated by a wide spectrum of AHLs that were previously found to be synthesized by bacteria and AHLs not yet found in bacteria, namely C_{15}- and C_{20}-HL. Whereas C_7-HL containing an acyl chain with an odd number of C-atoms did not stimulate DNA binding, C_{15}-HL also characterized by an odd-numbered acyl chain was active in the stimulation of DNA-binding activity. This suggests that the length of the acyl chain rather than an even or odd number of C-atoms is an important factor for the ability to stimulate the DNA-binding activity of ExpR. This effect was observed especially well at a single molecule level, where AFM force spectroscopy proved to be a sensitive tool for binding analysis of complex multiple-component systems. By this method, we also obtained evidence that C_7-HL binds to the ExpR protein but is not able to stimulate protein-DNA interaction. Furthermore, since the interaction of C_7-HL with ExpR appeared to prevent stimulation by C_{12}-HL, this points to the possibility of an inhibitory effect of AHLs synthesized by an endogenous AHL synthase other than SinI or by other bacteria. C_7-HL is a naturally occurring AHL produced by *Rhizobium leguminosarum* (43).

TABLE 2 Molecular interaction parameters for ExpR-DNA binding under various AHL effectors as derived from DFS

HL	Reaction length x_β (Å)	Off-rate k_{off} (s^{-1})	Mean lifetime (ms)
C_8	5.7 ± 0.3	0.48 ± 0.16	2273 ± 758
C_{10}	5.2 ± 0.3	1.43 ± 0.45	699 ± 220
C_{12}	2.9 ± 0.2	5.40 ± 1.03	185 ± 35
oxo-C_{14}	3.5 ± 0.3	3.48 ± 0.62	287 ± 51
$C_{16:1}$	3.9 ± 0.6	2.19 ± 1.88	457 ± 392
C_{18}	4.7 ± 0.8	1.32 ± 1.27	758 ± 729

The wide range of acyl chain lengths results in significant variations of solubilities and, therefore, makes it difficult to determine and to compare kinetic parameters of AHL-activated ExpR in ensemble experiments. DFS has proven to be particularly useful in this respect since only values determined for ExpR proteins activated by a bound AHL molecule can be taken into account. In this manner, kinetic parameters of the molecular interaction between DNA and AHL-activated ExpR were determined.

Both the lifetimes of the bound complexes and the length scales of the dissociation processes varied with different AHLs bound to the protein. This supports the hypothesis that

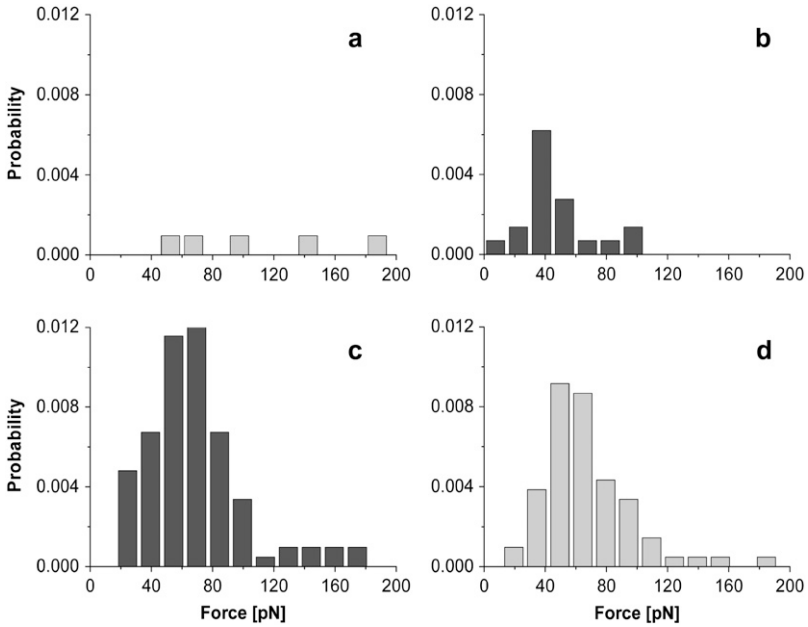

FIGURE 8 Stability of the protein-effector bond. (*a*) In the presence of C_7-HL, no binding is observed. (*b*) After the sample was washed multiple times with buffer solution over the course of 1 h and C_{12}-HL was added, the protein-DNA complex is still inactive. The reverse process was investigated with a new tip and sample surface: (*c*) In the presence of C_{12}-HL, the protein-DNA complex shows its usual degree of activity. (*d*) C_7-HL was added after the sample was washed multiple times over the course of 1 h. Activity is only slightly reduced. Obviously, C_7-HL is not able to displace C_{12}. Both experiments indicate a high stability of the protein-effector bond.

ExpR may regulate target genes differently in response to different SinI-dependent AHLs and is in agreement with previously reported specific ExpR-dependent effects of different AHLs on levels of proteins (13). It has been reported that diverse spectra of AHLs were synthesized in different culture media and growth phases (5,44). This may affect the availability of various AHLs for activation of the LuxR-type regulators under different growth conditions.

We obtained indirect evidence on the protein-effector interaction as well, implicating a very stable bond between ExpR and its associated AHLs. A tight interaction with their cognate AHLs was also reported for the *A. tumefaciens* TraR and the *V. fischeri* LuxR, although competition with halogenated furanones (42) and experiments showing that the LuxR-AHL complex can be reversibly inactivated by dilution (40,41) suggested a reversible binding of the signal molecules. Various LuxR-type regulators may exhibit differences in AHL accessibility and stability of the protein-AHL complex.

The DNA binding site of ExpR is located immediately upstream of a lux box-like sequence preceding the AHL synthase gene *sinI*. Since expression of *sinI* seems to be strongly dependent on *sinR* (5,45), it is possible that the lux box-like sequence constitutes the binding site of SinR. Hence SinR and ExpR may interact during binding to this DNA region.

Finally, we would like to stress the capacity of single molecule force experiments to analyze protein-DNA interactions with attention to molecular details of the binding mechanism: Evidently, a single C-atom more or less in the side chain of the AHL effector could make a big difference in functionality.

We thank M. Borgmann for RT-PCR *sinI* results.

This work was supported by SFB 613 from the Deutsche Forschungsgemeinschaft.

REFERENCES

1. Gonzalez, J. E., and M. M. Marketon. 2003. Quorum sensing in nitrogen-fixing rhizobia. *Microbiol. Mol. Biol. Rev.* 67:574–592.
2. Swift, S., J. A. Downie, N. A. Whitehead, A. M. Barnard, G. P. Salmond, and P. Williams. 2001. Quorum sensing as a population-density-dependent determinant of bacterial physiology. *Adv. Microb. Physiol.* 45:199–270.
3. Fuqua, C., M. R. Parsek, and E. P. Greenberg. 2001. Regulation of gene expression by cell-to-cell communication: acyl-homoserine lactone quorum sensing. *Annu. Rev. Genet.* 35:439–468.
4. Pearson, J. P., C. V. Delden, and B. H. Iglewski. 1999. Active efflux and diffusion are involved in transport of *Pseudomonas aeruginosa* cell-to-cell signals. *J. Bacteriol.* 181:1203–1210.
5. Marketon, M. M., and J. E. Gonzalez. 2002. Identification of two quorum-sensing systems in *Sinorhizobium meliloti*. *J. Bacteriol.* 184: 3466–3475.
6. Marketon, M. M., M. R. Groquist, A. Eberhard, and J. E. Gonzalez. 2002. Characterization of the *Sinorhizobium meliloti sinR/sinI* locus and the production of novel N-acyl homoserine lactones. *J. Bacteriol.* 184:5686–5695.
7. Pellock, B. J., M. Teplitski, R. P. Boinay, W. D. Bauer, and G. C. Walker. 2002. A LuxR homolog controls production of symbiotically active extracellular polysaccharide II by *Sinorhizobium meliloti*. *J. Bacteriol.* 184:5067–5076.
8. Hanzelka, B. L., and E. P. Greenberg. 1995. Evidence that the N-terminal region of the *Vibrio fischeri* LuxR protein constitutes an autoinducer-binding domain. *J. Bacteriol.* 177:815–817.
9. Vannini, A., C. Volpari, C. Gargioli, E. Muraglia, R. Cortese, R. De Francesco, P. Neddermann, and S. Di Marco. 2002. The crystal structure of the quorum sensing protein TraR bound to its autoinducer and target DNA. *EMBO J.* 21:4393–4401.
10. Stevens, A. M., K. M. Dolan, and E. P. Greenberg. 1994. Synergistic binding of the *Vibrio fischeri* LuxR transcriptional activator domain and RNA polymerase to the *lux* promoter region. *Proc. Natl. Acad. Sci. USA.* 91:12619–12623.

11. Marketon, M. M., S. A. Glenn, A. Eberhard, and J. E. Gonzalez. 2003. Quorum sensing controls exopolysaccharide production in *Sinorhizobium meliloti*. *J. Bacteriol.* 185:325–331.
12. Hoang, H., A. Becker, and J. E. Gonzalez. 2004. The LuxR homolog ExpR, in combination with the sin quorum sensing system, plays a central role in *Sinorhizobium meliloti* gene expression. *J. Bacteriol.* 186:5460–5472.
13. Gao, M., H. Chen, A. Eberhard, M. R. Gronquist, J. B. Robinson, B. G. Rolfe, and W. D. Bauer. 2005. sinI- and expR-dependent quorum sensing in Sinorhizobium meliloti. *J. Bacteriol.* 187:7931–7944.
14. Bustamante, C., J. C. Macosko, and G. J. Wuite. 2000. Grabbing the cat by the tail: manipulating molecules one by one. *Nat. Rev. Mol. Cell Biol.* 1:130–136.
15. Lee, G. U., L. A. Chrisey, and R. J. Colton. 1994. Direct measurement of the forces between complementary strands of DNA. *Science.* 266: 771–773.
16. Florin, E.-L., V. T. Moy, and H. E. Gaub. 1994. Adhesion forces between individual ligand-receptor pairs. *Science.* 264:415–417.
17. Hinterdorfer, P., W. Baumgartner, H. Gruber, K. Schilcher, and H. Schindler. 1996. Detection and localization of individual antibody-antigen recognition events by atomic force microscopy. *Proc. Natl. Acad. Sci. USA.* 93:3477–3481.
18. Dammer, U., M. Hegner, D. Anselmetti, P. Wagner, M. Dreier, W. Huber, and H.-J. Güntherodt. 1996. Specific antigen/antibody interactions measured by force microscopy. *Biophys. J.* 70:2437–2441.
19. Ros, R., F. Schwesinger, D. Anselmetti, M. Kubon, R. Schäfer, A. Plückthun, and L. Tiefenauer. 1998. Antigen binding forces of individually addressed single-chain Fv antibody molecules. *Proc. Natl. Acad. Sci. USA.* 95:7402–7405.
20. Evans, E., A. Leung, V. Heinrich, and C. Zhu. 2004. Mechanical switching and coupling between two dissociation pathways in a P-selectin adhesion bond. *Proc. Natl. Acad. Sci. USA.* 101:11281–11286.
21. Dammer, U., O. Popescu, P. Wagner, D. Anselmetti, H.-J. Güntherodt, and G. N. Misevic. 1995. Binding strength between cell adhesion proteoglycans measured by atomic force microscopy. *Science.* 267:1173–1175.
22. Bartels, F. W., B. Baumgarth, D. Anselmetti, R. Ros, and A. Becker. 2003. Specific binding of the regulatory protein ExpG to promoter regions of the galactoglucan biosynthesis gene cluster of *Sinorhizobium meliloti*—a combined molecular biology and force spectroscopy investigation. *J. Struct. Biol.* 143:145–152.
23. Koch, S. J. and M. D. Wang. 2003. Dynamic force spectroscopy of protein-DNA interactions by unzipping DNA. *Phys. Rev. Lett.* 91:208103-1–208103-4.
24. Kühner, F., L. T. Costa, P. M. Bisch, S. Thalhammer, W. M. Heckl, and H. E. Gaub. 2004. LexA-DNA bond strength by single molecule force spectroscopy. *Biophys. J.* 87:2683–2690.
25. Baumgarth, B., F. W. Bartels, D. Anselmetti, A. Becker, and R. Ros. 2005. Detailed studies of the binding mechanism of the Sinorhizobium meliloti transcriptional activator ExpG to DNA. *Microbiology.* 151: 259–268.
26. Eckel, R., S. D. Wilking, A. Becker, N. Sewald, R. Ros, and D. Anselmetti. 2005. Single-molecule experiments in synthetic biology: an approach to the affinity ranking of DNA-binding peptides. *Angew. Chem. Int. Ed. Engl.* 44:3921–3924.
27. Evans, E., and K. Ritchie. 1997. Dynamic strength of molecular adhesion bonds. *Biophys. J.* 72:1541–1555.
28. Merkel, R., P. Nassoy, A. Leung, K. Ritchie, and E. Evans. 1999. Energy landscapes of receptor-ligand bonds explored with dynamic force spectroscopy. *Nature.* 397:50–53.
29. Meade, H. M., S. R. Long, G. B. Ruvkun, S. E. Brown, and F. M. Ausubel. 1982. Physical and genetic characterization of symbiotic and auxotrophic mutants of Rhizobium meliloti induced by transposon Tn5 mutagenesis. *J. Bacteriol.* 149:114–122.
30. Glazebrook, J., and G. C. Walker. 1989. A novel exopolysaccharide can function in place of the calcofluor-binding exopolysaccharide in nodulation of alfalfa by Rhizobium meliloti. *Cell.* 56: 661–672.
31. Beringer, J. E. 1974. R factor transfer in *Rhizobium leguminosarum*. *J. Gen. Microbiol.* 84:188–198.
32. Schirmer, F., S. Ehrt, and W. Hillen. 1997. Expression, inducer spectrum, domain structure and function of MopR, the regulator of phenol degradation in *Acinetobacter calcoaceticus*. *J. Bacteriol.* 179: 1329–1336.
33. Newman, J. R., and C. Fuqua. 1999. Development of an alternative controlled expression system for diverse bacteria: use of an araC-PBAD cassette to analyze quorum sensing in Agrobacterium tumefaciens. *Gene.* 227:197–203.
34. Simon, R., U. Priefer, and A. Pühler. 1983. A broad host range mobilization system for in vivo genetic engineering: transposon mutagenesis in Gram negative bacteria. *Biotechnology.* 1:783–791.
35. Oikawa, Y., K. Sugano, and O. Yonemitsu. 1978. Meldrums acid in organic-synthesis. 2. General and versatile synthesis of beta-keto-esters. *J. Org. Chem.* 43:2087–2088.
36. Becker, A., H. Berges, L. Krol, C. Bruand, S. Rüberg, E. Capela, E. Lauber, E. Meilhoc, F. Ampe, F. J. de Bruijn, J. Fourment, A. Francez-Charlot, D. Kahn, H. Küster, C. Liebe, A. Pühler, S. Weidner, and J. Batut. 2004. Global changes in gene expression in Sinorhizobium meliloti 1021 under microoxic and symbiotic conditions. *Mol. Plant Microbe Interact.* 17:292–303.
37. Hutter, J. L., and J. Bechhoefer. 1993. Calibration of atomic-force microscope tips. *Rev. Sci. Instrum.* 7:1868–1873.
38. Slock, J., D. VanRiet, D. Kolibachuk, and E. P. Greenberg. 1990. Critical regions of the *Vibrio fischeri* LuxR protein defined by mutational analysis. *J. Bacteriol.* 172:3974–3979.
39. Becker, A., S. Rüberg, H. Küster, A. A. Roxlau, M. Keller, T. Ivashina, H. P. Cheng, G. C. Walker, and A. Pühler. 1997. The 32-kilobase exp gene cluster of Rhizobium meliloti directing the biosynthesis of galactoglucan: genetic organization and properties of the encoded gene products. *J. Bacteriol.* 179:1375–1384.
40. Urbanowski, M. L., C. P. Lostroh, and E. P. Greenberg. 2004. Reversible acyl-homoserine lactone binding to purified *Vibrio fischeri* LuxR protein. *J. Bacteriol.* 186:631–637.
41. Zhu, J., and S. C. Winans. 2001. The quorum-sensing transcriptional regulator TraR requires its cognate signaling ligand for protein folding, protease resistance, and dimerization. *Proc. Natl. Acad. Sci. USA.* 98:1507–1512.
42. Manefield, M., R. de Nys, N. Kumar, R. Read, M. Givskov, P. Steinberg, and S. Kjelleberg. 1999. Evidence that halogenated furanones from Delisea pulchra inhibit acylated homoserine lactone (AHL)-mediated gene expression by displacing the AHL signal from its receptor protein. *Microbiology.* 145:283–291.
43. Lithgow, J. K., A. Wilkinson, A. Hardman, B. Rodelas, A. Wisniewski-Dye, P. Williams, and J. A. Downie. 2000. The regulatory locus *cinRI* in *Rhizobium leguminosarum* controls a network of quorum-sensing loci. *Mol. Microbiol.* 37:81–97.
44. Teplitski, M., A. Eberhard, M. R. Gronquist, M. Gao, J. B. Robinson, and W. D. Bauer. 2003. Chemical identification of N-acyl homoserine lactone quorum-sensing signals produced by Sinorhizobium meliloti strains in defined medium. *Arch. Microbiol.* 180:494–497.
45. Llamas, I., N. Keshavan, and J. E. Gonzalez. 2004. Use of *Sinorhizobium meliloti* as an indicator for specific detection of long-chain *N*-acyl homoserine lactones. *Appl. Environ. Microbiol.* 70: 3715–3723.